Soil texture and water retention as spatial predictors of denitrification in urban wetlands

Monica M. Palta,[1*] Joan G. Ehrenfeld,[2**] Daniel Gimenez,[3] Peter M. Groffman,[4] Vandana Subroy[3]

[1]Arizona State University, School of Earth and Space Exploration, P.O. Box 876004, Tempe, AZ 85287, USA; phone: 480-727-2551, fax: 480-965-8102; mpalta@asu.edu

[2]Rutgers University, Department of Ecology & Evolution, 14 College Farm Road, New Brunswick, NJ 08901, USA

[3]Rutgers University, Department of Environmental Sciences, 14 College Farm Road, New Brunswick, NJ 08901, USA

[4]City University of New York, Advanced Science Research Center, 85 St. Nicholas Terrace, New York, NY 10031, USA

[*]Corresponding author

[**]Deceased

ABSTRACT

Urban wetlands potentially play an important role in nitrate (NO_3^-) removal from stormwater, but nitrogen loading from the atmosphere and surface water must intersect with soil properties optimal for NO_3^- removal for this potential to be realized. We examined predictors of NO_3^- removal via the microbial process of denitrification in an urban wetland system in New Jersey, USA with highly heterogeneous soils. Soil cores representing the wide range of soil textures at the site were collected to examine relationships between intact core denitrification rates, denitrification enzyme activity (DEA), available inorganic nitrogen, and soil water retention characteristics. Water retention curves were characterized for pressure potentials ranging from -1 to -5000 cm and used to estimate pore size distribution parameters. The highest intact core denitrification rates occurred in soils located at low elevations, with high macroporosity, and low variability in soil pore radius. High DEA corresponded with high available soil NO_3^- and high elevation. Soil samples collected at 118 points from the site and analyzed for soil organic matter and texture fractions were used to create interpolated raster layers of properties related to high denitrification rates ("hot spots"). Weighted estimations of whole-site NO_3^- removal based on denitrification hot spots were higher than site estimations based on average denitrification rates, suggesting that studies using the latter approach may be underestimating NO_3^- removal at the landscape level. Stormwater channels at the site intersected with denitrification hot spots over 20% of total channel area, indicating that soils may be at least partially reducing total NO_3^- loads to the adjacent creek. These results show that soil physical properties that are relatively immutable can be used for predicting the location of potential hot spots of microbial activity at the landscape scale.

Key words: Denitrification; nitrification; water retention; pore size distribution; biogeochemical hot spots; urban stormwater

1. Introduction

The ability of floodplain and wetland soils to retain and/or reduce nutrients through microbial processing is important, due to concerns about nutrient loading and eutrophication in adjacent waterways (Ehrenfeld et al., 2003; Paerl et al., 2006; Paul and Meyer, 2001; Walsh et al., 2005). Wetland restoration and construction is increasingly used as a means of reducing inorganic nitrogen, especially nitrate (NO_3^-), in agricultural and urban runoff. However, reliable estimates of whole-site NO_3^- removal potential that are based on drivers of microbial activity in the soils and sediments of urban watersheds and associated wetland environments are needed to design or manage these systems effectively for the maximum reductive capacity. Nitrate removal via denitrification is a microbial process performed by a diverse group of heterotrophic and some autotrophic bacteria that are ubiquitous in the environment (Robertson and Groffman, 2015). These microbes use NO_3^- as an electron acceptor and convert it to gaseous forms, with N_2 as the final product in the reaction sequence. This process has been identified by environmental scientists and managers as a desirable way of converting a highly biologically reactive and potential ecologically damaging form of nitrogen (NO_3^-) to a highly inert form (N_2) that is already pervasive in the environment (Davidson et al., 2012).

Quantification and prediction of denitrification in soils is difficult. Denitrification occurs under sub-oxic (<0.2 mg O_2/L, Seitzinger et al., 2006) conditions and requires NO_3^- (produced by nitrification under aerobic conditions) and labile carbon. The availability of these substrates and conditions are in turn controlled by a complex set of environmental variables, which exhibit high levels of spatial and temporal variability (Seitzinger et al., 2006). Although we know that hydrology is an important mediator of substrates and redox status in wetland soils, a number of variables can influence and interact with hydrologic regimes. Soil structure and texture

69 determine pore connectivity and water-filled pore space, which in turn influences nutrient
70 cycling within and between soil microsites (Castellano et al., 2013; Groffman and Tiedje, 1991;
71 Morse et al., 2012; Parkin, 1987). Compacted soils with high clay content and low porosity
72 appear to lack adequate exchange of substrates between aerobic and sub-oxic pores to couple
73 nitrification and denitrification (Palta et al., 2014). On the other hand, given adequate soil
74 moisture, high porosity and low tortuosity in coarser soils seem to facilitate exchange between
75 pores supporting NO_3^- creation via nitrification and pores supporting NO_3^- removal via
76 denitrification (Palta et al., 2014). Topographic positioning can affect drainage of a soil, and
77 poorly drained, sub-oxic soils can either support high (Aulakh and Rennie, 1985; Groffman and
78 Tiedje, 1989a, 1989b) or low (Palta et al., 2014) rates of denitrification, depending on NO_3^-
79 availability.
80 Attempts to characterize the dynamic controls of water and soil physical properties on
81 microbial processes, including nitrogen gas production, have often focused on water filled pore
82 space as an integrated predictor (e.g., Linn and Doran, 1984). A more comprehensive
83 characterization of these dynamics requires quantification of a water retention curve that defines
84 the relationship between the water content, θ, and the soil water potential, ψ (van Genuchten,
85 1980), but this is rarely done. Different soils often exhibit distinctive water retention curves,
86 providing a basis for characterizing landscape variation in soil moisture dynamics.
87 The urban environment presents a unique challenge for predicting whole-site soil
88 denitrification rates or denitrification potential. Studies examining urban and suburban sites in a
89 variety of metropolitan areas have found significant effects of the urban environment on soil
90 nitrogen and carbon pools and storage, but these effects vary considerably across the urban
91 landscape due to patchiness of land use, vegetation, and soil types (Sawa et al., 2010). Urban

92 soils are often composed of a mixture of materials differing from those of natural soils and/or are
93 deeply modified in physical structure and chemical composition by human activity (De Kimpe
94 and Morel, 2000); this makes prediction of soil microbial process rates as a function of soil
95 structural components challenging. Here, we studied an urban floodplain site with a high level
96 of spatial heterogeneity in soil texture and structure, hydrology, and topography (Palta et al.,
97 2014). As with much of urban land, this site has a long history of human activity and
98 modification. These heterogeneous soil conditions have important implications for soil
99 chemistry and microbial processes.
100 A number of studies have identified both the pressing need for scaling denitrification
101 information from small-scale point measurements to large (meters to kilometers) spatial scales,
102 and the difficult challenge of scaling a process that is so highly variable at the microbial scale
103 (Boyer et al., 2006; Groffman et al., 2009; Kulkarni et al., 2008; Van Breemen et al., 2002).
104 Because small areas (hot spots) often account for a high percentage of N gas flux activity
105 (Anderson et al., 2015; Duncan et al., 2013; Parkin, 1987), scaling point measurements to
106 landscape or watershed scales must involve identifying these areas and their drivers, particularly
107 for estimates of whole-site or whole-system N removal (Kulkarni et al., 2008; Tague et al., 2010;
108 Vidon et al., 2010). The purpose of this study was (1) to identify the soil physical characteristics
109 that best predict the highest (hot spots) and lowest (cold spots) actual and potential rates of
110 denitrification within a small wetland complex in a park located on an abandoned urban site, and
111 (2) use the spatial positioning of these characteristics relative to the location of stormwater flow
112 to estimate whole-site potential for NO_3^- removal. We collected over 100 soil samples along
113 transects through the site to characterize soil particle size distribution and organic matter content,
114 and measured denitrification rates, denitrification potential and water retention characteristics on

115 19 of these samples. The latter subset was selected to represent the broad range of soil textures
116 at the site. Previous research conducted at 14 locations in the same study site demonstrated that
117 soil denitrification is tightly coupled to soil nitrification, and that soil porosity and connectivity
118 likely facilitate this coupling (Palta et al., 2014).

119 We expected that the highest denitrification rates would be found in areas with water
120 retention characteristics supporting simultaneous nitrification and denitrification within the soil
121 matrix. We therefore hypothesized that soils with high macroporosity, intermediate water-
122 holding capacity and pore sizes, and intermediate elevations would demonstrate the highest rates
123 of denitrification at the site. Potential denitrification rates are measured in slurries under
124 anaerobic conditions, where soil structure plays less of a role in mediating the redox status of
125 pores and delivery of NO_3^- to denitrifiers. We therefore expected that potential denitrification
126 rates would be mediated less by soil structure and more by NO_3^- availability and overall size and
127 activity of the denitrifier community. Consequently, we hypothesized that the highest potential
128 denitrification rates would occur at intermediate soil available NO_3^- concentrations, since very
129 anaerobic soils have low NO_3^- production and therefore low denitrifier activity and populations,
130 and very aerobic soils have high NO_3^- production, but bacterial populations have little need to
131 produce denitrifying enzymes. Lastly, we expected that stormwater flowpaths mainly intersected
132 with low elevation areas that are semi-permanently flooded, and therefore too anaerobic to
133 support denitrification activity. Thus, we hypothesized that whole-site potential removal of NO_3^-
134 in stormwater would be low.
135

136 **2. Materials and Methods**

137 *2.1. Site Description*

138 The study took place in the Teaneck Creek wetland complex, a small (0.2 km^2) freshwater
139 floodplain ecosystem in northeastern New Jersey (NJ) that is part of the larger Hackensack River
140 watershed (Fig. 1). Teaneck Creek is a former brownfield area, and most soils at the site are
141 classified as Udorthents, organic substratum, 0–8% slopes (Soil Survey Staff, 1999). Soils in
142 this category are filled and smoothed or otherwise extensively disturbed to a depth of 1 meter or
143 more, with buried tidal marsh deposits underneath, but are too variable in their properties to be
144 classified to the next level. Soils located at an elevation of 4 meters or more on the Eastern side
145 of the site (Fig. 1) are classified as Dunellen-Urban land complex, 15–25% slopes (Soil Survey
146 Staff, 1999). These are coarse-loamy, mixed, active, mesic Typic Hapludults: very deep, well-
147 drained soils, found on outwash plains and stream terraces. The numerous geomorphologic,
148 biological, and hydrologic alterations at the site have led to high variation in soil profile
149 composition at very small spatial scales, with soil textures ranging from clays to pure sand and
150 gravel due to the varied history of land use at the site (see supplemental material).
151 The location and movement of standing water through the site has also changed substantially
152 since the late 1890s. The site has remained at a lower elevation than the surrounding landscape
153 (Fig. 1), but the deposition of dredge and other materials has resulted in areas within the site that
154 are drier than they were historically; i.e. they rarely support standing water. The stream has been
155 channelized and re-routed into the eastern side of the site. As a result, some areas that were
156 previously characterized by anaerobic, waterlogged soils are now aerobic and well-drained.
157
158 *2.2. Soil Physical Characteristics*
159 Soil samples were collected during summer 2007. Eight transects were designed to traverse
160 the site in a west to east direction, and two points at each elevation (i.e., within each 0.61 m

contour on a topographic map) were identified across each transect; this resulted in soils being collected from 118 points. Elevation data were obtained from a 0.61 m digital elevation model of the site (B2A SURVSAT 2003). Mid-sections of a few of the transects were not accessible due to excessive flooding at the time of sampling or very dense and tangled vegetation covering large mounds of debris (Fig. 1). Samples with volumes ranging from 3.5 to 7.5 L of soil were collected from the top 10 cm of the profile at each point using shovels. Within 24 h of collection, a subsample was taken from each sample and dried at 105°C for 48 h. Percent organic matter of oven-dried soil subsamples was then determined using loss on ignition of soil at 450 °C for 4 h (Nelson and Sommers, 1996). The remainder of each sample was air-dried in the laboratory for two weeks.

Particle size distributions with 11 size fractions (sand: 2, 1, 0.7, 0.5, 0.25, 0.1, 0.053 mm; silt: 20-50, 5-20, 2-5 μm; clay: <2 μm) were determined using the pipette method (Gee and Bauder, 2006) on 90 samples with organic matter contents of less than 20%; the 28 remaining samples with organic matter contents ≥20% were eliminated from this analysis.

Particle size distributions were characterized with the geometric mean diameter (MPS) and the geometric standard deviation (σ_p) estimated from the mass fractions contained in each of the size classes according to Shirazi & Boersma (1984):

$$MPS = exp\,[\sum m_i x\,] \quad (1)$$

$$\sigma_p = exp\,[[\sum m_i x^2 - \ln(MPS)^2\,]^{1/2}] \quad (2)$$

where m_i is the mass fraction of the textural fraction i and x is the natural log transformed particle size of the textural fraction i. Additionally, the parameters MPS and σ_p were used to calculate the entropy of particle size distributions, SH_p according to:

$$SH_p = \ln(\mathrm{MPS}) + 0.5 + 0.5 * \ln\,(2 * \pi * {\sigma_p}^2) \quad (3)$$

184 Where SH_p assumes a log-normal distribution of particle sizes (Yoon and Gimenez, 2012).

185

186 *2.3. Soil denitrification and inorganic nitrogen measurements*

187 Soil samples to characterize denitrification rates and inorganic nitrogen content were
188 collected on two different days in August and in September 2009. Nineteen sample sites were
189 selected from the original 118 sample sites to represent the range of textures found at the site
190 (Fig. 2), from loamy sand (83% sand, 13% silt, 0% clay) to silt loam (20% sand, 60% silt, 15%
191 clay) to silty clay loam (7% sand, 59% silt, 34% clay).

192 Intact cores were collected from each of the 19 sites using a 20x3 cm corer and analyzed for
193 denitrification rate using the acetylene block method immediately upon returning to the lab (less
194 than 8 h) using procedures outlined in Groffman et al. (1999). The intact core method is
195 designed to mimic field conditions as closely as possible, and is suitable for landscape-scale
196 studies, as it allows for large numbers of samples to be run simultaneously (Groffman et al.,
197 1999). Acetylene inhibits N_2O to N_2 reduction, making N_2O the terminal product of all
198 denitrification in a soil (Groffman et al., 1999). Production of N_2O is more easily detected than
199 N_2 production, due to the high atmospheric background signal of N_2 (Groffman et al., 2006).

200 Upon returning to lab, intact cores were made airtight with rubber stoppers and vented (i.e.,
201 headspace was composed of ambient lab air at atmospheric pressure). Five mL acetylene gas
202 (equivalent to 10–12% of headspace volume) was added to the core headspace, and was mixed
203 into soil pores by pumping the core three times with a 40 mL syringe. Gas samples were taken at
204 2 and 6 h using a syringe and stored in evacuated glass tubes at 23°C until they could be
205 analyzed for N_2O by electron capture gas chromatography on a Shimadzu 14A GC-ECD. The
206 headspace of each chamber was mixed prior to each sampling by pumping with a 40 mL syringe

three times. Soil moisture was maintained at ambient (field) levels during incubation for denitrification analysis. Incubation temperatures during denitrification analysis were the same and within 5°C, respectively, of field temperatures on the two sampling days.

Intact soil cores were stored (less than 24 h) at 4°C between denitrification analysis and analysis for extractable NO_3^- and NH_4^+, gravimetric moisture content, and soil organic matter using procedures modified from Robertson et al. (1999). Soil samples were hand sorted and mixed, and held at field moisture for NO_3^- and NH_4^+ extraction with 2M KCl followed by colorimetric analysis with an Omnion Lachat Quickchem 8000 (Lachat Instruments, Loveland, CO). Soil moisture content was determined by drying soil at 105°C for 48 h. Soil organic matter content was determined as described above. Soil moisture content, determined by oven drying at 105°C for 48 h, did not differ, on average, between the two dates (data not shown).

For the September collection date, denitrification rate was measured on intact cores and potential denitrification rate, or denitrification enzyme activity (DEA), was measured with soil slurries. Replicate cores were collected at each sample site on the same date. Intact core denitrification rate was measured on one set of replicate cores in the lab within 8 h of collection using the methods described above. The second set of replicate cores were stored at 4°C for one week, and then used to measure potential denitrification rate in the following manner: soil core samples were brought to room temperature (23°C), hand sorted and mixed, and subsampled for determination of extractable NO_3^-, extractable NH_4^+, gravimetric moisture content, and percent organic matter using the methods described above. Replicate slurries of each sample (1:1 g soil:mL distilled water) were prepared and placed in airtight 250 mL flasks, and the headspace was made anaerobic by evacuating and flushing vials 5 times with N_2 gas. After the 5th evacuation, the headspace was brought to ambient pressure with N_2 gas. Acetylene gas (10 mL,

230 or 11–16% of headspace volume) was injected into each vial, slurries were placed on a rotating
231 table, and 10 mL of headspace was sampled after 30 and after 90 min using a syringe. Samples
232 were stored in evacuated glass tubes at 23°C until they could be analyzed for N_2O on a Shimadzu
233 14A GC-ECD.
234
235 *2.4. Water Retention Curves*
236 Soil cores (3 cm in height and 5.4 cm in diameter) were collected (in duplicate) in 2009 at 18
237 of the 19 sites used in the denitrification analysis and analyzed for water content at pressure
238 potentials ranging from -1 to -50 cm using the hanging water column method (Dane and
239 Hopmans, 2002). The replicate sample from one of the sites was damaged during transportation
240 to the laboratory, and was not analyzed. Cores were saturated for approximately 24 hours, then
241 placed in chambers on saturated double-layered Whatman #3 filter paper (Whatman, Clifton NJ,
242 USA) and equilibrated at successively decreasing pressure potentials of -1, -5, -10, -20 and -50
243 cm, until outflow from the cores was negligible. The total outflow at each pressure potential was
244 measured for each core individually. At the end of the experiment, soil cores were removed
245 from the system and 10 g of soil was removed from the top and the bottom of the core, and dried
246 separately at 105°C for 24 h; the average of the two samples was used to determine gravimetric
247 water content at equilibrium with -50 cm potential.
248 The volume of the soil samples used in the hanging column system was measured by filling
249 the space between the soil surface and the rim of the core with warm paraffin and determining its
250 volume by the gain in core weight divided by the density of paraffin wax (0.91 g/cm^3). Soil
251 volume in the core, calculated by subtracting the volume of the added paraffin from the volume
252 of the core (68.67 cm^3), was used to calculate bulk density, which in turn, was used to convert

253 gravimetric to volumetric water content. Volumetric water content at -50 cm potential was
254 calculated from gravimetric water content at the end of the experiment; water contents at all
255 other pressure potentials were back-calculated from this value using the outflow volume from the
256 core over each change in pressure potential.
257 Water retention curves at pressure potentials of -320 cm, -1000 cm, or -5000 cm were
258 determined with a pressure plate extractor system (Soilmoisture Equipment Corp., Santa
259 Barbara, CA, USA) using sub-samples from soil cores (5 cm in height, 8 cm in diameter)
260 collected from the 18 sites along with the smaller cores used in the hanging column analysis.
261 Three subsamples were taken from the top and the bottom of each large core using metal rings
262 (0.6 cm in height, 2.4 cm in diameter). Following sub-sampling, gravimetric water content of the
263 cores was estimated by sampling a total of about 20 g removed in equal amounts from the top
264 and bottom of the cores and drying at 105°C for 24 h. Gravimetric water content of the cores
265 was used to calculate dry bulk density. Bulk densities calculated in this manner were
266 comparable to bulk densities calculated using the paraffin method in the previous analysis (data
267 not shown). Ceramic plates were covered with a paste of diatomaceous earth and then layered
268 with wet filter paper before setting down the subsamples, which were placed in shallow water to
269 saturate overnight. Samples were equilibrated for 17 d at pressure potentials of -320 cm and -
270 1000 cm, and for 27 d at -5000 cm.
271 Water retention data were fitted with the van Genuchten (1980) and the Kosugi (1996)
272 models using the SWRC Fit (Seki, 2007) online program (http://swrcfit.sourceforge.net) to
273 estimate parameters for the van Genuchten (1980) model, i.e. water content at saturation (θ_s), the
274 residual water content (θ_r), α, and n. Water content at the inflection point of the water retention
275 curve (θ_p) was calculated from these parameters using the equation from Dexter (2004):

276 $$\theta_p = \theta_r + (\theta_s - \theta_r) * (1 + \left(\frac{n}{n-1}\right))^{(\frac{1}{n} - 1)} \quad (4)$$

277 The SWRC Fit program also calculates parameters for the lognormal model for water
278 retention, i.e. θ_s, θ_r, h_m, and σ (Kosugi, 1996). This model assumes a lognormal pore size
279 distribution, where σ is a dimensionless parameter corresponding to the standard deviation of
280 log-transformed soil pore radius, and h_m (cm) is the pressure potential related to the geometric
281 mean pore radius, r_m. When h_m is expressed in units of cm and r_m in units of μm, r_m can be
282 estimated from the absolute value of h_m as $r_m = 1490/|h_m|$.

283 Several parameters were calculated to characterize pore structure of the soil from estimated
284 parameters of both the van Genuchten and the Kosugi models. Effective porosity was calculated
285 as θ_s - θ_p, and macroporosity, or the fraction of total pore space composed of the largest
286 conducting pores, was calculated as (θ_s - θ_p) / θ_s. The parameters for these calculations were
287 obtained from the estimated van Genuchten model. Soil entropy (SH), a unified index of pore
288 distribution, was calculated using parameters estimated by the lognormal Kosugi model as (Yoon
289 and Giménez, 2012):

290 $$SH = (\theta_s - \theta_r) * \ln(r_m) + 0.5 + 0.5 * \ln(2 * \pi * \sigma^2) - (\theta_s - \theta_r) * \ln(\theta_s - \theta_r) \quad (5)$$

291

292 *2.5. Statistical Analysis*

293 Cluster analysis (K-means) was used to uncover which soil physical and chemical
294 characteristics tended to co-occur with high denitrification rates (IBM Corp., 2012). To address
295 the original hypotheses that soils with high macroporosity, intermediate water-holding capacity
296 and pore size, and intermediate elevations would demonstrate the highest rates of denitrification
297 in the site, three cluster analyses were run: The first included all nitrogen cycling data, to test
298 whether any general patterns emerged between inorganic nitrogen content of soil and intact core

and potential denitrification rates. The second examined the relationship between denitrification rate in intact cores, soil available NO_3^-, and soil physical characteristics potentially regulating NO_3^- production, i.e., pore characteristics (SH, h_m, σ, effective porosity, macroporosity), particle distribution (MPS, % clay, σ_p, SH_p), and elevation. The third analysis used the same variables as in the second analysis, but instead of intact core denitrification rates, potential denitrification rate as indicated by denitrification enzyme activity (DEA) was the response variable.

A hierarchical cluster analysis (IBM Corp., 2012) was used to determine how many clusters were to be used for each of the k-means cluster analyses. Because cluster analysis cannot accommodate missing values and denitrification rate values were missing for a few samples collected in August 2009, 12 of the original 19 samples were used in the cluster analyses for this date. Cluster center values of predictive variables (NO_3^-, soil physical characteristics) were then regressed against cluster center values of denitrification rates using curve estimation in SPSS (IBM Corp., 2012).

2.6. Spatial Analysis

Following cluster analysis to determine which soil characteristics co-occurred with high or low denitrification rates, maps were interpolated for these characteristics using the point data on soil texture fractions, elevation, and organic matter data collected at the site in 2005–2006 (16 total) and 2007 (118 total) (Fig. 1). These maps were constructed to determine the location and extent of hot spots of denitrification at the whole-site level and whether these hot spots coincided with areas of NO_3^- loading (i.e., stormwater flowpaths). Texture fractions were used to estimate soil structural variables, described in further detail in the Results section.

321 Soil characteristics at the site are highly related spatially to human use (i.e., to where
322 materials were dumped). To improve the spatial accuracy of the interpolated data, historic urban
323 land use was captured by digitizing aerial photography of the site from 1966 (following the
324 heaviest dumping activity at the site, and immediately preceding site abandonment) (Fig. 1, see
325 also supplemental material) (USGS-EROS 1966). The photograph was georeferenced in
326 ArcMap (ESRI, 2010) using 2007 aerial photography (NJ-OIT, Office of Geographic
327 Information Systems 2007), and then digitized into a polyline shape file by visually assessing
328 and delimiting areas of differing vegetation and areas with bare soil under different use (Fig. 1,
329 see supplemental material). This layer was used to constrain an inverse weighted distance
330 interpolation of soil properties derived from the point data (maximum search radius 150 m)
331 (ESRI, 2010), but was not used to constrain interpolations of soil organic matter, since the latter
332 soil property was likely to be more related to vegetation and flooding than to previous land use.
333 Stormwater channels conveying water into and through the site were digitized as a polyline
334 shapefile using 2007 aerial photography and converted to a raster layer (1.5 m cell size) (ESRI,
335 2010). A sampling analysis was used to determine the total area over which these flowpaths
336 intersected with given soil physical characteristics and elevations of interest (ESRI, 2010). The
337 layers used for this analysis included the digital elevation model of the site, and the interpolated
338 layers of soil properties (see Section 2.7).
339
340 *2.7. Denitrification Mapping and Validation*
341 Based on cluster and regression analysis, σ, macroporosity, elevation, and extractable soil
342 NO_3^- were the strongest predictors of intact core denitrification rates (see Results). Since we
343 analyzed 105 samples of the 134 samples collected at the site during 2005–2007 for soil texture

344 and organic matter, but not extractable NO_3^-, water retention, or bulk density (Fig. 1), we needed
345 a means of approximating soil properties predictive of either low (cold spots) or high (hot spots)
346 intact core denitrification across the watershed using our texture and organic matter data. Using
347 the macroporosity and σ values calculated for the 18 samples analyzed for water retention
348 characteristics, and values of parameters reflecting particle size distribution (percent sand,
349 percent silt, percent clay, SH_p, and σ_p) and percent OM for 105 samples collected at the site
350 during 2005–2007, we performed a multiple imputation in SPSS to replace missing
351 macroporosity and σ values for the entire data set (IBM Corp., 2012). In multiple imputation,
352 missing values are predicted using existing values from other variables; uncertainty is accounted
353 for by creating different versions of the missing data and observing the variability between
354 imputed data sets. We ran 20 imputations using a linear regression with a fully conditional
355 (Markov chain Monte Carlo or MCMC) specification method using 1000 iterations. The fully
356 conditional method is recommended for an arbitrary pattern of missing values (IBM Corp.,
357 2012). Once macroporosity and σ datasets were created for 105 points, layers for both variables
358 were then interpolated for the entire site using an inverse distance weighted (IDW) analysis
359 (ESRI, 2010).
360 A 2006 study at the same site examining denitrification rates at 14 points over three seasons
361 found that soils defined as "organic-rich" (percent organic matter > 15%, on average) were found
362 to support low rates of denitrification (i.e., these soils constituted "cold spots"), due to the fact
363 that these soils were semi-permanently flooded, and supported low endogenous NO_3^- production
364 (Palta et al. 2014, see Table 1). We interpolated a layer for soil organic matter using inverse
365 weighted distance (minimum number of points = 5) for use in assessing where high

366 macroporosity was unlikely to sustain high levels of denitrification (i.e., where soil organic
367 matter was > 15%).
368 To assess how accurately our map predicted denitrification hot and cold spots, we compared
369 known hot or cold spots identified in the 2006 study to our interpolated hot/cold spot layer. Hot
370 and cold spots in the 2006 study were defined by how often the denitrification rate at each site
371 exceeded the 3rd quartile value (30.3 μg N kg^{-1} d^{-1}) of the data distribution (Table 1, Palta et al.,
372 2014). Cold spots (hereafter referred to as points 1–6) were the "organic-rich" soils mentioned
373 above. Hot spots, or areas exceeding the 3rd quartile value of the data distribution most often (in
374 this case, in at least one-third of measurements, hereafter referred to as points 7–12) were loam
375 soils with the highest rates of denitrification in 2006. Clay soils (hereafter referred to as points
376 13 and 14) demonstrated intermediate rates of denitrification in 2006.
377
378 **3. Results**
379 *3.1. Soil textural characteristics*
380 Of the 118 sites sampled in 2007 (Fig. 1), 24% of the samples had in organic matter contents
381 greater or equal to 20% OM and were therefore not analyzed for texture. The remaining 90
382 samples were primarily loams ranging in texture from loamy sand, at the more coarse-grained
383 end of the textural spectrum, to silty clay loam at the more fine-grained end of the textural
384 spectrum (Fig. 2). Percent organic matter in the soils ranged from 0.2–47.9% (Table 2). 21% of
385 the 90 samples analyzed for texture met the definition of an "organic soil," i.e., between 12 and
386 18% organic matter by weight when percent clay in the soil is between 0 and 60% (SMSS,
387 1988).
388

389 *3.2. Regulation of denitrification rates by soil physical variables and nitrate availability*

390 Hierarchical cluster analysis of nitrogen cycling data over the entire study period indicated
391 five distinct clusters (Table 3). Hierarchical cluster analysis of intact core and potential
392 denitrification rates, respectively, with soil structural data indicated four distinct clusters for each
393 cluster analysis (Tables 4&5). All correlation analysis results were obtained by regressing
394 cluster center values against one another. K-means cluster analysis indicated a strong quadratic
395 relationship between cluster center values of intact core (R^2=0.744, p<0.01) and potential
396 (R^2=0.982, p=0.02) denitrification rate and soil available NO_3^-, although the highest rates of
397 potential and intact core denitrification were not consistently predicted by the same range of
398 NO_3^- values (Table 3). NO_3^- was one of the strongest predictors (R^2=0.620, p=0.02) of intact
399 core denitrification rate cluster center values, with a significantly negative relationship between
400 denitrification rate and NO_3^- rather than a quadratic relationship as found in the first cluster
401 analysis. In the third cluster analysis, soil available NO_3^- generated one of the strongest models
402 for predicting potential denitrification rate, although NO_3^- values were not significantly different
403 between clusters according to an ANOVA (Table 5). Potential denitrification rate demonstrated
404 a strong (but insignificant) positive quadratic correlation with available NO_3^- (R^2=0.931, p=NS),
405 with the highest potential denitrification rates coinciding with the highest soil available NO_3^-
406 (Table 5). Available NO_3^- did demonstrate a marginally significant (p=0.15) linear relationship
407 with potential denitrification rate cluster centers, but the R^2 was lower for the linear model
408 (R^2=0.727) than for the quadratic model (Table 5).

409 Other strong predictors of intact core denitrification rate cluster center values were σ
410 (R^2=0.694, p=0.05), percent macropores (R^2=0.693, p=0.05), and elevation (R^2=0.676, p=0.06),
411 although clusters were not significantly different from one another in elevation according to an

412 ANOVA (Table 4). As hypothesized, percent macropores demonstrated a significant positive
413 linear relationship with intact core denitrification rate in the second cluster analysis, although this
414 relationship was quadratic (Table 4). Comparison of the water retention curves for soil samples
415 representing each of the macroporosity cluster center values demonstrates high variability in
416 volumetric water content at low (-1 to -100 cm) pressure potentials (Fig. 3). However, at
417 pressure potentials lower than -100 cm, the volumetric water contents in samples with
418 macroporosities of 31 and 35% were slightly lower than in samples with macroporosities of 24
419 and 30% (Fig. 3). Macroporosity was also strongly negatively correlated with NO_3^- cluster
420 values (Fig. 4). Elevation and σ (related to the standard deviation of the pore radius)
421 demonstrated marginally significant and significant quadratic relationships, respectively, with
422 intact core denitrification rates, with the lowest elevation and σ values corresponding to the
423 highest intact core denitrification rates (Table 4). The clusters for h_m were marginally
424 significantly different ($p=0.07$) from each other according to an ANOVA, and h_m demonstrated a
425 weaker ($R^2=0.593$), marginally significant ($p=0.10$) quadratic relationship with intact core
426 denitrification rate (Table 4).

427 As hypothesized, aspects of soil structure regulating NO_3^- production and availability that
428 were important in regulating denitrification rates in intact cores were not generally strongly
429 correlated with potential denitrification rates (Table 5). Most variables in the third k-means
430 cluster analysis did not demonstrate significant differences between clusters according to an
431 ANOVA (Table 5). However, elevation did show a marginal significant difference ($p=0.13$)
432 between clusters, and marginally significant quadratic ($R^2=0.982$, $p=0.13$) and linear ($R^2=0.841$,
433 $p=0.08$) relationships with potential denitrification rate (Table 5). Potential denitrification rate,
434 unlike intact core denitrification rate, was lowest at low elevations and highest at high elevations

435 (Table 5). Effective porosity did demonstrate a marginally significant (p=0.15) linear
436 relationship with potential denitrification rate cluster centers, but the R^2 was lower for the linear
437 model (R^2=0.716) than for the quadratic model (Table 5).
438
439 *3.3. Scaling Up Denitrification Hot Spots to the Landscape Level*
440 Macroporosity and σ values imputed by multiple imputation analysis matched the original
441 data (2009) sample data well in terms of mean, standard deviation, and range of values (Table 2).
442 The imputed ranges of values for macroporosity and σ were, however, slightly higher and lower,
443 respectively, than the original dataset. The interpolated layers of σ and macroporosity accurately
444 predicted σ and macroporosity for the 19 points sampled in 2009, as interpolated values
445 correlated strongly with measured values (σ: R=0.984, p<0.001; macroporosity: R=0.943,
446 p<0.001).
447 The interpolated layer of organic matter predicted areas of "organic-rich" soils (as defined by
448 Palta et al. 2014) fairly well, based on field observations and actual measurements at points 1, 2,
449 5, and 6 (Fig. 5). It did not capture some of the organic-rich soil areas near Teaneck Creek (Fig.
450 5), possibly because these areas were flooded and therefore not well-sampled in the 2007 field
451 sampling (Fig. 1).
452 Based on the results of the cluster analysis, sites included in clusters C and D of the 2nd
453 cluster analysis were defined as hot spots of denitrification (see Discussion). In situ
454 denitrification levels were therefore assumed to be highest in areas with elevations < 2.66 m,
455 with σ values < 1.98, and with macroporosities > 0.30 (Table 4). When σ, macroporosity,
456 elevation, and soil organic matter layers were combined, they yielded a map predicting hot spots
457 of denitrification at the site (Fig. 5). The interpolated layer of hot spots accurately captured hot

458 spot point measurements from 2006 (points 7–12) and correctly identified points 1, 2, 5, 6, 13
459 and 14 as cold spots. Points 3 and 4 were incorrectly identified as potential areas of high
460 denitrification, but these points were located near the edge of interpolated hot areas, within 5–6
461 meters of cold areas (Fig. 5).

462 Soil conditions facilitating hot spots of denitrification (σ values < 1.98, elevations < 2.66 m;
463 macroporosity > 0.30; organic matter < 15%) constituted 18% of the interpolated site (Fig. 6).
464 Samples in clusters C and D of the 2nd cluster analysis demonstrated an average intact core
465 denitrification rate of 137.8 μg NO_3^--N m^{-2} hr^{-1}, while samples in clusters A and B demonstrated
466 no measureable denitrification, on average. If the average denitrification rate for clusters C and
467 D is multiplied by total hot spot area, this translates to a potential removal rate of roughly 43.5
468 kg NO_3^--N yr^{-1} via denitrification across the entire site. If a whole-site estimate is made using
469 average denitrification rate across all samples (i.e., clusters A, B, C, and D), the whole site
470 potentially removes only 4.33 kg NO_3^--N yr^{-1} via denitrification.

471 Atmospheric loading rate of inorganic N to the site is approximately, on average, 43.4 μg N
472 m^{-2} hr^{-1} (24.9 μg NO_3^--N m^{-2} hr^{-1}) (Turpin et al., 2006). Denitrification rates in all sites in
473 clusters C and D of the 2nd cluster analysis exceeded 24.9 μg NO_3^--N m^{-2} hr^{-1} on at least one of
474 the two sampling dates; on the second sampling date, all samples in both clusters C and D
475 exceeded 24.9 μg NO_3^--N m^{-2} hr^{-1}. All but one of the sites in clusters C and D also exceeded
476 43.4 μg N m^{-2} hr^{-1} on at least one of the two sampling dates. None of the samples in either the A
477 or B clusters exceeded 24.9 μg NO_3^--N m^{-2} hr^{-1} on either date, save one.

478 Stormwater channels intersected areas with conditions constituting denitrification hot spots
479 over roughly 20% of total stormwater channel length. Measurements in the headwaters of
480 Teaneck Creek have estimated a loading rate of 0.4–58.1 kg NO_3^- per day from surface water

481 (http://cues.rutgers.edu/teaneck-creek-conservancy/data/). The total channel area digitized in
482 this analysis was 4,240 m^2; 3,154 m^2 of this was stormwater channels feeding Teaneck Creek.
483 Using these numbers, loading through the stormwater channels is approximately 1.2–173.3 μg
484 NO_3^--N m^{-2} hr^{-1} during water flow through the channels, making total loading to any given point
485 along the stormwater channels (from atmospheric deposition and stormwater) approximately
486 27.9–200.0 μg NO_3^--N m^{-2} hr^{-1}. Points in cluster C of the 2nd cluster analysis had denitrification
487 rates greater than 27.9 μg N m^{-2} hr^{-1} during one or both sampling dates, but never equaled or
488 exceeded 200.0 μg NO_3^--N m^{-2} hr^{-1}. One point in cluster D of the 2nd cluster analysis exceeded
489 200.0 μg NO_3^--N m^{-2} hr^{-1} on both sampling dates.
490
491 **4. Discussion**
492 Measuring or estimating biogeochemical processes at the ecosystem scale is nearly always
493 contingent on defining and predicting hot spots, which can be difficult without intensive
494 biogeochemical field measurements over space and time. Denitrification is mediated by
495 biogeochemical dynamics in soil that are typically heterogeneous over time and space. This
496 variation can be difficult to predict, particularly in urban environments, where soil conditions are
497 created or modified by human activity. We were able to use soil physical properties as a basis
498 for (1) defining denitrification hot spots, (2) extrapolating point measurements of soil properties
499 moderating denitrification rates to the site scale, and (3) evaluating the importance of
500 denitrification as a sink for atmospheric deposition and stormwater loading of inorganic N at the
501 site scale.
502
503 *4.1. Soil physical properties regulate denitrification rate*

504 As hypothesized, the highest intact core denitrification rates were found in soils with water
505 retention characteristics facilitating simultaneous nitrification and denitrification. These sites
506 had low σ (i.e., low standard deviation of log-transformed soil pore radius), high macroporosity,
507 low elevation, and low NO_3^-. Our results suggest, as hypothesized, that high elevation sites
508 produce high NO_3^- but are too aerobic to support high denitrification rates. As expected, the first
509 cluster analysis (Table 3), which included all nitrogen cycling data to test whether any general
510 patterns emerged between inorganic nitrogen content of soil and intact core and potential
511 denitrification rates, supported the idea of a quadratic relationship between extractable NO_3^- and
512 both intact core and potential denitrification rates. The second cluster analysis, which examined
513 relationships between denitrification rate in intact soil cores and soil available NO_3^- and soil
514 physical characteristics, demonstrated a linear negative correlation between extractable NO_3^- and
515 intact core denitrification rates, and a quadratic relationship with elevation, with the lowest
516 elevations supporting the highest denitrification rates (Table 4). The third cluster analysis, which
517 examined the relationship between potential denitrification rate in anaerobic slurries and soil
518 available NO_3^- and soil physical characteristics, found quadratic relationships between potential
519 denitrification rates and extractable NO_3^- and elevation, with the highest potential denitrification
520 rates occurring at high NO_3^- concentrations and high elevations (Table 5). These results all
521 support the idea that, at high elevations, where NO_3^- is in high supply, anaerobic conditions are
522 the most limiting factor for denitrification. It is surprising that intact core denitrification rates
523 did not drop at the lowest elevations as expected, but we did not sample semi-permanently
524 flooded areas of the site in this study, where previous work has found endogenous NO_3^-
525 production and denitrification rate to be low under very wet conditions (Palta et al. 2014).

526 Further, the relationship between intact core denitrification rates and elevation was quadratic,
527 which suggests that at even lower elevations, denitrification rates may start declining.
528 Cluster center values for intact core denitrification rate were slightly different between the
529 first and second cluster analysis. This was likely due to the fact that soils analyzed for potential
530 denitrification rate demonstrated different ranges and microbial community response (i.e., high
531 vs. low activity) than when analyzed in intact cores. These inconsistencies in rate under the two
532 types of analyses were expected and have been found in a number of other studies examining
533 both potential and intact core denitrification rates (Groffman and Tiedje, 1989b; Groffman, 1987;
534 Simek et al., 2004; Smith and Parsons, 1985). The highest intact core denitrification rates were
535 supported by low end of the range of soil NO_3^- concentrations (0–4,000 µg NO_3^--N/kg soil),
536 while the soil slurries used in the DEA analysis demonstrated the highest rates in the high end of
537 the range of soil NO_3^- concentrations (5,000–13,000 µg NO_3^--N/kg soil). These differences
538 between potential and intact core denitrification rates and predictors are likely due to differences
539 in analytical techniques between intact core and DEA analysis. Extractable NO_3^- was sampled
540 from soils prior to analyzing them for potential denitrification rate, whereas in the case of intact
541 cores, extractable NO_3^- was sampled from soils after measuring intact core denitrification rate.
542 Extractable NO_3^- in the case of the potential denitrification rate analysis is therefore likely to be
543 more indicative of NO_3^- available to denitrifiers in the soil. Additionally, there are more
544 anaerobic conditions and fewer limitations to NO_3^- diffusion in the DEA analysis (Myrold and
545 Tiedje, 1985). In intact cores, NO_3^- forms in aerated pores and diffuses slowly through the pore
546 matrix to the anaerobic pores that support denitrifier activity. In soils with the higher soil NO_3^-
547 content, denitrifier communities are likely inhibited by the presence of oxygen and/or slow NO_3^-

548 diffusion. In the anaerobic slurries, oxygen does not inhibit denitrifier activity, and soils with
549 high NO_3^- content provide more substrate than soils with low NO_3^- content.
550 DEA is a good estimate of the activity of denitrification enzymes in the soil in the absence of
551 diffusion limitations. However, intact core denitrification, in which the pore structure of the soil
552 is kept relatively intact, more accurately represents activity of the denitrifier community in situ.
553 Intact core measurements are therefore a better means for identifying hot spots of denitrification
554 at the watershed scale, while DEA is more useful as a comparative measurement between soil
555 types, or as a measure of limitations to enzyme activity (Groffman et al., 2006, 1999). Since
556 denitrification at the study site appeared to be tightly coupled to nitrification in the soil, our
557 intact cores measurements of denitrification using acetylene potentially underestimated actual
558 denitrification rates, due to acetylene inhibition of nitrification (Duncan et al., 2013; Groffman et
559 al., 1999; Morse et al., 2015). However, we attempted to minimize this problem by incubating
560 the cores quickly (within eight hours of collection), and for a short time (six hours total).
561 Variables related to soil pore structure and drainage, as predicted, had significant correlations
562 with intact core denitrification rates. Potential denitrification rates, as expected, demonstrated no
563 significant correlations with soil physical variables (Table 5). Uniformity of pore radius (i.e., σ)
564 yielded the best model for predicting cluster center values for intact core denitrification, with
565 more uniform pore distributions supporting the highest denitrification rates (Table 4).
566 Macroporosity had a positive significant quadratic relationship with intact core denitrification
567 rate, and yielded the best model after σ (Table 4). The strong negative correlation found between
568 macroporosity and soil extractable NO_3^- in the second correlation analysis (Fig. 4) is likely the
569 outcome of soils with high macroporosity supporting coupled nitrification-denitrification. These
570 high macroporosity soils likely have adequate aerobic pore space to produce NO_3^- yet were

571 located at low enough elevations to support water-filled anaerobic pore space capable of fueling
572 high NO_3^- consumption via denitrification (Table 4). Low macroporosity soils tend to remain
573 wetter than high macroporosity soils when subjected to the same tension during a drying phase
574 (Fig. 3), which impedes oxygen diffusion into the soil (van der Weerden et al., 2012). Previous
575 studies have found that soils classified as "poorly drained," due to a high relative soil moisture
576 (gravimetric or volumetric water content), high percentage of fine textured soil particles, high
577 microporosity, low macroporosity, low elevation, and/or a combination thereof, demonstrate
578 higher denitrification or N_2O production rates than better-drained or well-drained soils (Aulakh
579 and Rennie, 1985; Groffman and Tiedje, 1989a, 1989b; van der Weerden et al., 2012). However,
580 in these studies, NO_3^- was generally not limiting: one study utilized agricultural soils (Aulakh
581 and Rennie, 1985), another measured denitrification rates under N additions (van der Weerden et
582 al. 2012), and in the remaining studies, soil fertility was higher in the poorly drained soils than in
583 the better-drained soils (Groffman and Tiedje, 1989a, 1989b). Pinay et al. (2007) examined
584 forested alluvial soils in multiple plots in seven river systems across Europe, and determined that
585 soil moisture, temperature, and NO_3^- (in order of decreasing importance) were the three main
586 control variables of intact core denitrification rates at the European scale (Pinay et al., 2007). As
587 in our study, intact core denitrification rates demonstrated a negative relationship with soil NO_3^-,
588 and a quadratic relationship with soil moisture, with intermediate values (between 60% and 80%
589 of maximum soil moisture) supporting the highest rates of denitrification (Pinay et al., 2007).
590
591 *4.2. Soil physical properties can be used to predict denitrification hot spots*
592 Biogeochemical hot spots are defined as areas "show[ing] disproportionately higher reaction
593 rates" relative to "the surrounding matrix" (McClain et al., 2003). Many studies take a more

qualitative approach to determining which rates are "highest" in a given set of data (Dai et al., 2012; Gu et al., 2012; Johnston et al., 2001; Tzoraki et al., 2007; Vidon et al., 2010; Zhu et al., 2012), but recent studies examining hot spots in landscapes have emphasized using the distribution of measured data to define hot spots in a particular spatial context (Darrouzet-Nardi and Bowman, 2011; Harms and Grimm, 2008; Johnson et al., 2010; Palta et al., 2014). Our 2006 study at this research site defined hot spots as sampling points that exceeded the 3rd quartile value (30.3 μg $N\text{-}N_2O$ kg^{-1} d^{-1}) of measured denitrification rates at the site significantly more often than other sampling points (Palta et al. 2014). The 2006 study found a lower range of denitrification rates (-43.3–364.9 μg $N\text{-}N_2O$ kg^{-1} d^{-1}) than this study (-695.7–1590.5 μg $N\text{-}N_2O$ kg^{-1} d^{-1}), but the 3rd quartile value for the denitrification rate measurements in this study was 84.8 μg $N\text{-}N_2O$ kg^{-1} d^{-1}, over twice as high as the 3rd quartile value in the 2006 study. This difference in range is likely because the sites in the 2009 study were located in areas with soil conditions associated with high rates of denitrification in the 2006 study. In the 2006 study, loam soils in fill piles exceeded 3rd quartile values more than any other soils, and "organic-rich" soils (>15% soil organic matter, flooded on nearly all sample dates) only exhibited "hot" rates on a few occasions (Table 1). Of the 19 sites used in 2009, 16 (84%) were some type of loam, two were loamy fine sand, and none were from areas defined as "organic-rich" (Fig. 2).

One potential limitation of defining hot spots based on an existing data distribution, rather than using a pre-defined range, is that due to sampling constraints and limitations, it is unlikely that the distribution of a given set of data will capture the full range of rates occurring at a site under myriad environmental conditions (Darrouzet-Nardi and Bowman, 2011). Because our 2006 denitrification data set included a greater range of spatiotemporal conditions, namely, more hydrogeological settings (flooded as well as unflooded areas) and denitrification measurements

over three seasons (376 measurements total), the data distribution from the 2006 data set may be more useful for identifying "hot" areas of the landscape. In the 2009 sampling, intact core denitrification rates of samples in clusters C and D (Table 4) exceeded 30.3 μg $N\text{-}N_2O$ kg^{-1} d^{-1} (the 2006 3rd quartile value) on one or both sample dates in all cases except one. Just under half the samples in clusters C and D (three out of eight) exceeded 84.8 μg $N\text{-}N_2O$ kg^{-1} d^{-1} (the 2009 3rd quartile value) on one or both sample dates. None of the denitrification rates in clusters A and B (Table 4) exceeded 30.3 μg $N\text{-}N_2O$ kg^{-1} d^{-1} or 84.8 μg $N\text{-}N_2O$ kg^{-1} d^{-1} on either date. Based on these criteria, we defined the sites in clusters A and B as cold spots and the sites in clusters C and D as hot spots of denitrification. Twelve of the 14 plots monitored in 2006 were correctly identified as either hot or cold spots of denitrification, indicating that the map is likely a good representation of heterogeneity in denitrification rates across the site. The plots monitored in 2006 were 3 meters x 3 meters in dimension, and were within six meters of cold areas on the map. The two areas incorrectly identified as hot spots on the map may therefore be due to minor spatial inaccuracies generated during interpolation of point data.

The mapping results suggest that using soil physical variables that are relatively static in space and time as a basis for quantifying and mapping the distribution of hot spots is a useful approach to addressing high variability in biogeochemical processes such as denitrification. Identifying the factors most limiting to denitrification (NO_3^-, O_2, organic C, or a combination thereof) is critical to determining which soil physical variables may be of highest importance in driving high denitrification rates, and these will not be consistent across all sites (Seitzinger et al., 2006). For example, in watersheds or wetland complexes that have much higher inputs of NO_3^- (e.g., in agricultural settings or in areas receiving sewage or treated wastewater), the presence of soil organic matter (Rotkin-Ellman et al., 2004), high soil moisture (McPhillips and

640 Walter, 2015), or high water residence time (McPhillips et al., 2015) may be a bigger
641 determinant of denitrification hot spots. In cases of low soil moisture and high soil O_2
642 availability, groundwater seeps (Burgin et al., 2010; Kaur et al., 2016) or the presence of
643 standing water (Capps et al., 2014) may determine denitrification hot spots in riparian areas. In
644 wetland landscapes such as described in this study, however, where carbon and low oxygen
645 environments are in abundance, soil pore characteristics mediating coupled nitrification and
646 denitrification are likely to be important determinants of denitrification hot spots (Palta et al.,
647 2014, 2013; Seitzinger et al., 2006; Shrestha et al., 2012).
648
649 *4.3. Denitrification in Brownfield Soils is Mitigating Inorganic Nitrogen Pollution*
650 Our estimation of whole-site NO_3^- removal using denitrification hot spots (43.5 kg NO_3^--N
651 yr^{-1}) demonstrated significant potential removal of NO_3^- from stormwater and the atmosphere in
652 an urban brownfield watershed. Our estimate of whole-site NO_3^- removal using average
653 denitrification rates across all samples (hot and cold spots) was ten times lower than that of the
654 estimate using hot spots, indicating that whole-site or whole-system calculations that are not
655 spatially weighted may be underestimating whole-site NO_3^- removal. The whole-site estimate
656 using hot spots assumes that the average intact core denitrification rate across hot spots measured
657 on our two sample dates would apply throughout the entire year, which is unlikely to be the
658 case—temperature and soil water, for example, are likely to cause significant outliers from this
659 average rate throughout the year (Palta et al., 2014). However, even if we only assume that hot
660 spots exceed 30.3 μg $N\text{-}N_2O$ kg^{-1} d^{-1} (the 2006 3rd quartile value) during one-third of the year
661 (the minimum criteria for a hot spot at the site according to Palta et al. (2014)), whole-site NO_3^-

662 removal would be, at minimum, 5.20 kg NO_3^--N yr^{-1}; this value is still higher than an estimate
663 based on the average denitrification rate of all samples (i.e., 4.33 kg NO_3^--N yr^{-1}).
664 Since intact core denitrification rates in sites in clusters C and D of the 2nd cluster analysis
665 matched or exceeded atmospheric loading of NO_3^- (43.6 kg NO_3^--N yr^{-1}) and total inorganic N
666 (76.0 kg N yr^{-1}), this suggests that approximately one-fifth of the site has the potential to
667 denitrify all atmospheric deposition of inorganic N. We expected that stormwater flowpaths
668 mainly intersected with low elevation areas that are semi-permanently flooded, and therefore too
669 anaerobic to support denitrification activity. However, stormwater channels intersected areas
670 with conditions constituting hot spots roughly 20% of the time, indicating that NO_3^--laden
671 surface flow may not be entirely bypassing areas capable of removing stormwater NO_3^- via
672 denitrification. We do not yet know whether the highest rates of activity at these hot spots
673 coincide with loading events (i.e., whether "hot moments" of denitrification align with NO_3^-
674 loading). Further, our analysis did not take into account the residence time of stormwater in a
675 given area of soil, which is a critical determinant of the capability of sediments to remove
676 surface water NO_3^- (Seitzinger et al., 2006). More detailed analysis of hydrologic residence
677 times would improve our assessments of the potential of these wetlands to denitrify NO_3^- in
678 stormwater and could form the basis for design and management actions to facilitate this activity
679 in this and other urban wetlands (Collins et al., 2010). Previous work has shown, however, that
680 experimentally flooding soils from the site with concentrations of NO_3^- similar to that of
681 measured field values in stormwater can significantly increase denitrification rates in the soils
682 (Palta et al., 2014). These results suggest that hot moments should occur when hot spots receive
683 inputs of NO_3^-.

684 Although urban brownfield sites like this one may be serving as a significant sink for
685 atmospheric NO_3^- and/or NO_3^- in stormwater, it is important to note that because we utilized the
686 acetylene block method to measure denitrification rates, we have no way of determining whether
687 denitrification at the site is complete in its reaction sequence, i.e., resulting in the production of
688 N_2 (complete) rather than N_2O (incomplete). Because N_2O is a potent greenhouse gas (USEPA,
689 2006), management plans that seek to mitigate NO_3^- in stormwater and atmospheric deposition
690 by capitalizing on denitrification hot spots in a watershed must also confirm that these areas are
691 producing low net N_2O:N_2 ratios (Palta et al., 2013).
692
693 **CONCLUSIONS**
694 Soil properties (pore distribution, elevation, organic matter content) related to the ability of a
695 soil to simultaneously support nitrification and denitrification led to the highest rates of
696 denitrification across a brownfield wetland site. These results suggest that using soil physical
697 variables that are relatively static in space and time as a basis for quantifying and mapping the
698 distribution of hot spots is a useful approach to addressing high variability in biogeochemical
699 processes such as denitrification. Mapping the distribution of these variables in relation to
700 stormwater channels may be a useful approach for improving the capacity of urban wetlands to
701 prevent the movement of NO_3^- to receiving waters. Identifying soil structural properties in
702 brownfield floodplain soils associated with high denitrification rates provided a useful and
703 potentially more accurate way of estimating whole-site denitrification potential and could be
704 used to design management plans by which NO_3^-–laden stormwater can be routed through areas
705 with the ability to remove NO_3^-. Spatial analysis accurately predicted most locations of
706 denitrification hot spots and cold spots, but the high level of heterogeneity in soils and

topography at the site meant that smaller-scale variations (in organic matter, for example) were not always fully captured. This study demonstrates that even highly modified and unrestored sites in urban areas may be playing an important role in nitrogen cycling within these ecosystems, and that soil physical properties can be used for predicting the location of potential hot spots of denitrification at the landscape scale.

ACKNOWLEDGEMENTS

This work is dedicated to Joan Ehrenfeld, an inspired and innovative scientist. The authors thank Ciara Burkett and Roxanne Siegrist for extensive assistance with sample processing and analysis. Cathleen McFadden, Kai Li, Lucy McKeon, and Katie Tarsiewicz provided additional assistance with sample collection and analysis. Funding for this work was provided by the &$Ā !" Ā$% #Ā+2'(5'4)Ā*..063,-1Ā120+2/ Ā the New Jersey Water Resources Research Institute FY2007 Program – Project ID 2007NJ145B (USGS Grant Award Number 06HQGR0100), and by a grant from the CGIAR Research Program on Water, Land, and Ecosystems to Dr. Daniel Giménez. Ā

REFERENCES CITED

Anderson, T.R., Groffman, P.M., Walter, M.T., 2015. Using a soil topographic index to distribute denitrification fluxes across a northeastern headwater catchment. JOURNAL OF HYDROLOGY 522, 123–134. doi:10.1016/j.jhydrol.2014.12.043

Aulakh, M.S., Rennie, D.A., 1985. Gaseous nitrogen losses from conventional and chemical summer fallow. Canadian Journal of Soil Science 65, 195–203.

Boyer, E.W., Alexander, R.B., Parton, W.J., Li, C.S., Butterbach-Bahl, K., Donner, S.D., Skaggs, R.W., Del Gross, S.J., 2006. Modeling denitrification in terrestrial and aquatic ecosystems at regional scales. Ecological Applications 16, 2123–2142.

Burgin, A.J., Groffman, P.M., Lewis, D.N., 2010. Factors regulating denitrification in a riparian wetland. Soil Science Society of America Journal 74, 1826–1833.

Capps, K.A., Rancatti, R., Tomczyk, N., Parr, T.B., Calhoun, A.J.K., Hunter Jr., M., 2014. Biogeochemical Hotspots in Forested Landscapes: The Role of Vernal Pools in Denitrification and Organic Matter Processing. ECOSYSTEMS 17, 1455–1468. doi:10.1007/s10021-014-9807-z

Castellano, M.J., Lewis, D.B., Kaye, J.P., 2013. Response of soil nitrogen retention to the interactive effects of soil texture, hydrology, and organic matter. Journal of Geophysical Research Biogeosciences 118, 280–290.

Collins, K.A., Lawrence, T.J., Stander, E.K., Jontos, R.J., Kaushal, S.S., Newcomer, T.A., Grimm, N.B., Cole Ekberg, M.L., 2010. Opportunities and challenges for managing nitrogen in urban stormwater: A review and synthesis. Ecological Engineering 36, 1507–1519.

Dai, Z., Trettin, C., Li, C., Li, H., Sun, G., Amatya, D., 2012. Effect of assessment scale on spatial and temporal variations in CH4, CO2 and N2O fluxes in a forested wetland. Water, Air, & Soil Pollution 223, 253–265. doi:10.1007/s11270-011-0855-0

Dane, J., Hopmans, J., 2002. Water retention and storage, in: Dane, J.H., Topp, G.C. (Eds.), Methods of Soil Analysis, Part 4, Physical Methods. Soil Science Society of America, Madison, WI, pp. 675–720.

Darrouzet-Nardi, A., Bowman, W., 2011. Hot spots of inorganic nitrogen availability in an alpine-subalpine ecosystem, Colorado front range. Ecosystems 14, 848–863. doi:10.1007/s10021-011-9450-x

Davidson, E.A., David, M.B., Galloway, J.N., Goodale, C.L., Haeuber, R., Harrison, J.A., Howarth, R.W., Jaynes, D.B., Lowrance, R.R., Nolan, B.T., Peel, J.L., Pinder, R.W., Porter, E., Snyder, C.S., Townsend, A.R., Ward, M.H., 2012. Excess nitrogen in the U.S. environment: Trends, risks, and solutions. Issues in Ecology 15, 1–16.

De Kimpe, C.R., Morel, J.L., 2000. Urban soil management: A growing concern. Soil Science

165, 31–40.

Dexter, A.R., 2004. Soil physical quality - Part III: Unsaturated hydraulic conductivity and general conclusions about S-theory. Geoderma 120, 227–239. doi:10.1016/j.geoderma.2003.09.006

Duncan, J.M., Band, L.E., Groffman, P.M., 2013. Towards closing the watershed nitrogen budget: Spatial and temporal scaling of denitrification. Journal of Geophysical Research Biogeosciences 118, 1105–1119.

Ehrenfeld, J.G., Cutway, H.B., Hamilton, R.I., Stander, E., 2003. Hydrologic description of forested wetlands in northeastern New Jersey, USA - An urban/suburban region. Wetlands 23, 685–700. doi:10.1672/0277-5212(2003)023[0685:hdofwi]2.0.co;2

ESRI, 2010. ArcGIS 10.0.

Groffman, P., Butterbach-Bahl, K., Fulweiler, R., Gold, A., Morse, J., Stander, E., Tague, C., Tonitto, C., Vidon, P., 2009. Challenges to incorporating spatially and temporally explicit phenomena (hotspots and hot moments) in denitrification models. Biogeochemistry 92, 49–77.

Groffman, P.M., 1987. Nitrification and denitrification in soil: A comparison of enzyme assay, incubation and enumeration methods. Plant and Soil 97, 445–450.

Groffman, P.M., Altabet, M.A., Bohlke, J.K., Butterbach-Bahl, K., David, M.B., Firestone, M.K., Giblin, A.E., Kana, T.M., Nielsen, L.P., Voytek, M.A., 2006. Methods for measuring denitrification: Diverse approaches to a difficult problem. Ecological Applications 16, 2091–2122.

Groffman, P.M., Holland, E.A., Myrold, D.D., Robertson, G.P., Zou, X., 1999. Denitrification, in: Robertson, G.P., Bledsoe, C.S., Coleman, D.C., Sollins, P. (Eds.), Standard Soil Methods for Long Term Ecological Research. Oxford University Press, New York, pp. 272–288.

Groffman, P.M., Tiedje, J.M., 1991. Relationships between denitrification, CO2 production and air-filled porosity in soils of different texture and drainage. Soil Biology and Biochemistry 23, 299–302.

Groffman, P.M., Tiedje, J.M., 1989a. Denitrification in north temperate forest soils - spatial and temporal patterns at the landscape and seasonal scales. Soil Biology & Biochemistry 21, 613–620.

Groffman, P.M., Tiedje, J.M., 1989b. Denitrification in north temperate forest soils: Relationships between denitrification and environmental factors at the landscape scale. Soil Biology & Biochemistry 21, 621–626.

Gu, C., Anderson, W., Maggi, F., 2012. Riparian biogeochemical hot moments induced by stream fluctuations. Water Resources Research 48, W09546. doi:10.1029/2011wr011720

794 Harms, T.K., Grimm, N.B., 2008. Hot spots and hot moments of carbon and nitrogen dynamics
795 in a semiarid riparian zone. Journal of Geophysical Research-Biogeosciences 113,
796 G101020. doi:G0102010.1029/2007jg000588

797 IBM Corp., 2012. IBM SPSS Statistics for Windows, Version 21.0.

798 Johnson, D.W., Glass, D.W., Murphy, J.D., Stein, C.M., Miller, W.W., 2010. Nutrient hot spots
799 in some Sierra Nevada forest soils. Biogeochemistry 101, 93–103.

800 Johnston, C.A., Bridgham, S.D., Schubauer-Berigan, J.P., 2001. Nutrient dynamics in relation to
801 geomorphology of riverine wetlands. Soil Science Society of America Journal 65, 557–77.

802 Kaur, A.J., Ross, D.S., Shanley, J.B., Yatzor, A.R., 2016. Enriched Groundwater Seeps in Two
803 Vermont Headwater Catchments are Hotspots of Nitrate Turnover. WETLANDS 36, 237–
804 249. doi:10.1007/s13157-016-0733-z

805 Kosugi, K., 1996. Lognormal distribution model for unsaturated soil hydraulic properties. Water
806 Resources Research 32, 2697–2703.

807 Kulkarni, M. V, Groffman, P.M., Yavitt, J.B., 2008. Solving the global nitrogen problem: it's a
808 gas! Frontiers in Ecology and the Environment 6, 199–206. doi:10.1890/060163

809 Linn, D.M., Doran, J.W., 1984. Effect of water filled pore space on carbon dioxide and nitrous
810 oxide production in tilled and nontilled soils. Soil Science Society of America Journal 48,
811 1267–1272.

812 McClain, M.E., Boyer, E.W., Dent, C.L., Gergel, S.E., Grimm, N.B., Groffman, P.M., Hart,
813 S.C., Harvey, J.W., Johnston, C.A., Mayorga, E., McDowell, W.H., Pinay, G., 2003.
814 Biogeochemical hot spots and hot moments at the interface of terrestrial and aquatic
815 ecosystems. Ecosystems 6, 301–312. doi:10.1007/s10021-003-0161-9

816 McPhillips, L., Walter, M.T., 2015. Hydrologic conditions drive denitrification and greenhouse
817 gas emissions in stormwater detention basins. ECOLOGICAL ENGINEERING 85, 67–75.
818 doi:10.1016/j.ecoleng.2015.10.018

819 McPhillips, L.E., Groffman, P.M., Goodale, C.L., Walter, M.T., 2015. Hydrologic and
820 Biogeochemical Drivers of Riparian Denitrification in an Agricultural Watershed. WATER
821 AIR AND SOIL POLLUTION 226. doi:10.1007/s11270-015-2434-2

822 Morse, J.L., Ardón, M., Bernhardt, E.S., 2012. Using environmental variables and soil processes
823 to forecast denitrification potential and nitrous oxide fluxes in coastal plain wetlands across
824 different land uses. Journal of Geophysical Research Biogeosciences 117, G02023.
825 doi:10.1029/2011jg001923

826 Morse, J.L., Durán, J., Groffman, P.M., 2015. Denitrification and greenhouse gas fluxes in a
827 northern hardwood forest: the importance of snowmelt and implications for ecosystem N
828 budgets. Ecosystems 18, 520–532.

Myrold, D.D., Tiedje, J.M., 1985. Diffusional constraints on denitrification in soil. Soil Science Society of America Journal 49, 651–657.

Nelson, D.W., Sommers, L.E., 1996. Total carbon, organic carbon, and organic matter, in: Sparks, D.L. (Ed.), Methods of Soil Analysis, Part 3 - Chemical Methods. Soil Science Society of America, Madison, WI, pp. 961–1010.

Paerl, H.W., Valdes, L.M., Peierls, B.L., Adolf, J.E., Harding, L.W., 2006. Anthropogenic and climatic influences on the eutrophication of large estuarine ecosystems. Limnology and Oceanography 51, 448–462.

Palta, M.M., Ehrenfeld, J.G., Groffman, P.M., 2014. “Hotspots'' and ”Hot Moments'' of Denitrification in Urban Brownfield Wetlands. ECOSYSTEMS 17, 1121–1137. doi:10.1007/s10021-014-9778-0

Palta, M.M., Ehrenfeld, J.G., Groffman, P.M., 2013. Denitrification and Potential Nitrous Oxide and Carbon Dioxide Production in Brownfield Wetland Soils. JOURNAL OF ENVIRONMENTAL QUALITY 42, 1507–1517. doi:10.2134/jeq2012.0392

Parkin, T.B., 1987. Soil microsites as a source of denitrification variability. Soil Science Society of America Journal 51, 1194–1199.

Paul, M.J., Meyer, J.L., 2001. Streams in the urban landscape. Annual Review of Ecology and Systematics 32, 333–365.

Pinay, G., Gumiero, B., Tabacchi, E., Gimenez, O., Tabacchi-Planty, A.M., Hefting, M.M., Burt, T.P., Black, V.A., Nilsson, C., Iordache, V., Bureau, F., Vought, L., Petts, G.E., Decamps, H., 2007. Patterns of denitrification rates in European alluvial soils under various hydrological regimes. Freshwater Biology 52, 252–266.

Robertson, G.P., Groffman, P.M., 2015. Nitrogen transformations, in: Paul, E.A. (Ed.), Soil Microbiology, Ecology, and Biochemistry, Fourth Edition. Academic Press, Amsterdam, pp. 421–446.

Robertson, G.P., Wedin, D., Groffman, P.M., Blair, J.M., Holland, E.A., Nadelhoffer, K.A., Harris, D., 1999. Soil carbon and nitrogen availability: Nitrogen mineralization, nitrification and carbon turnover, in: Robertson, G.P., Bledsoe, C.S., Coleman, D.C., Sollins, P. (Eds.), Standard Soil Methods for Long Term Ecological Research. Oxford University Press, New York, pp. 258–271.

Rotkin-Ellman, M., Addy, K., Gold, A.J., Groffman, P.M., 2004. Tree species, root decomposition and subsurface denitrification potential in riparian wetlands. Plant and Soil 263, 335–344.

Sawa, Y., Szlavecz, K., Pouyat, R.V., Groffman, P.M., Heisler, G., 2010. Effects of land use and vegetation cover on soil temperature in an urban ecosystem. Soil Science Society of America Journal 74, 469–480.

865 Seitzinger, S., Harrison, J.A., Bohlke, J.K., Bouwman, A.F., Lowrance, R., Peterson, B., Tobias,
866 C., Van Drecht, G., 2006. Denitrification across landscapes and waterscapes: A synthesis.
867 Ecological Applications 16, 2064–2090.

868 Seki, K., 2007. SWRC fit – a nonlinear fitting program with a water retention curve for soils
869 having unimodal and bimodal pore structure. Hydrology and Earth System Sciences 4, 407–
870 437.

871 Shrestha, J., Niklaus, P.A., Frossard, E., Samaritani, E., Huber, B., Barnard, R.L., Schleppi, P.,
872 Tockner, K., Luster, J., 2012. Soil Nitrogen Dynamics in a River Floodplain Mosaic.
873 JOURNAL OF ENVIRONMENTAL QUALITY 41, 2033–2045. doi:10.2134/jeq2012.0059

874 Simek, M., Elhottova, D., Klimes, F., Hopkins, D.W., 2004. Emissions of N2O and CO2,
875 denitrification measurements and soil properties in red clover and ryegrass stands. Soil
876 Biology and Biochemistry 36, 9–21.

877 Smith, M.S., Parsons, L.L., 1985. Persistence of denitrifying enzyme-activity in dried soils.
878 Applied and Environmental Microbiology 49, 316–320.

879 SMSS, 1988. Keys to Soil Taxonomy, SMSS Technical Monograph. Cornell University, Ithaca,
880 NY.

881 Soil Survey Staff, N.R.C.S., 1999. Web Soil Survey [WWW Document]. United States
882 Department of Agriculture.

883 Tague, C., Band, L., Kenworthy, S., Tenebaum, D., 2010. Plot- and watershed-scale soil
884 moisture variability in a humid Piedmont watershed. Water Resources Research 46,
885 W12541. doi:10.1029/2009wr008078

886 Turpin, B., Seitzinger, S., Ravit, B., 2006. A study to link atmospheric N deposition with surface
887 and ground water N and denitrification capabilities in an urban New Jersey wetland. New
888 Brunswick, NJ.

889 Tzoraki, O., Nikolaidis, N.P., Amaxidis, Y., Skoulikidis, N.T., 2007. Instream biogeochemical
890 processes of a temporary river. Environmental Science & Technology 41, 1225–31.

891 USEPA, 2006. Global mitigation of non-CO2 greenhouse gases. US Environmental Protection
892 Agency, Washington, DC.

893 Van Breemen, N., Boyer, E.W., Goodale, C.L., Jaworski, N.A., Paustian, K., Seitzinger, S.P.,
894 Lajtha, K., Mayer, B., Van Dam, D., Howarth, R.W., Nadelhoffer, K.J., Eve, M., Billen, G.,
895 2002. Where did all the nitrogen go? Fate of nitrogen inputs to large watersheds in the
896 northeastern USA. Biogeochemistry 57, 267–293.

897 van der Weerden, T.J., Kelliher, F.M., de Klein, C.A.M., 2012. Influence of pore size
898 distribution and soil water content on nitrous oxide emissions. Soil Research 50, 125–135.

899 van Genuchten, M., 1980. A closed-form equation for predicting the hydraulic conductivity of

unsaturated soils. Soil Science Society of America Journal 44, 892–898.

Vidon, P., Allan, C., Burns, D., Duval, T.P., Gurwick, N., Inamdar, S., Lowrance, R., Okay, J., Scott, D., Sebestyen, S., 2010. Hot spots and hot moments in riparian zones: Potential for improved water quality management. JAWRA Journal of the American Water Resources Association 46, 278–298.

Walsh, C.J., Roy, A.H., Feminella, J.W., Cottingham, P.D., Groffman, P.M., Morgan, R.P., 2005. The urban stream syndrome: current knowledge and the search for a cure. Journal of the North American Benthological Society 24, 706–723.

Yoon, S.W., Gimenez, D., 2012. Entropy characterization of soil pore systems derived from soil-water retention curves. Soil Science 177, 361–368.

Zhu, Q., Schmidt, J.P., Bryant, R., 2012. Hot moments and hot spots of nutrient losses from a mixed land use watershed. Journal of Hydrology 414, 393–404.

Table 1. Intact core denitrification rate summaries of soil samples collected during a 2006 study at the Teaneck Creek Conservancy site. Samples were collected for each site (3 m x 3 m plots) for 27 days over 3 seasons. Soil texture and percent organic matter (OM) were measured on soils within each plot, and flooding (whether standing water was present at 5 cm below the soil surface or higher) was noted on each sampling day (Palta et al. 2014). Minimum and maximum denitrification rates are in μg N kg^{-1} d^{-1}. A denitrification rate of 30.3 μg N kg^{-1} d^{-1} was the 3rd quartile denitrification rate for all samples collected during the 2006 study.

	Denitrification Rate					
Site	Minimum	Maximum	% rates exceeding 30.3 μg N kg^{-1} d^{-1}	Soil Texture	Soil OM (%)	Days Flooded (%)
1	-11.9	1.76	0	Silty Loam	13.0±0.9	100
4	-4.61	2.21	0	Loam	17.6±1.2	100
5	-6.92	6.42	0	Silty Loam	19.3±0.9	93
3	-18.1	14.9	0	Silty Loam	18.2±0.9	100
2	-5.13	43.8	4	Sandy Loam	19.5±1.0	100
6	-8.77	66.8	4	Loam	13.1±1.0	100
14	-8.97	61.1	7	Clay	6.9±0.3	100
13	-4.52	110.5	31	Clay	7.2±0.5	0
7	-5.23	299.7	33	Sandy Loam	6.2±0.4	0
10	-0.51	287.5	37	Loam	13.0±0.5	0
12	-14.8	175.3	42	Clay Loam	9.8±0.5	0
11	-43.3	248.9	56	Loam	8.6±0.4	7
9	1.85	311.6	67	Loam	14.0±0.5	4
8	-0.56	364.9	70	Loam	10.8±0.4	21

928 **Table 2.** Measured physical and chemical characteristics of soils collected at the Teaneck Creek
929 Conservancy site, 2005–2009. Mean values are shown below ranges in parentheses. In the case
930 of percent macropores and σ, mean values are shown ± the standard deviation of the mean.
931

	Physical Characteristics			N Cycling
	2005–2007*	2005–2006**	2009‖	2009
% Organic Matter	0.3–47.9 (13.5)	8.7–47.9 (18.8)		
Mean Particle Size (μm)	2.6–349.6 (62.4)	32.7–349.6 (144.1)	30.0–720.0 (239.0)	
Elevation (m)	0–5.87 (2.80)		1.22–5.19 (2.70)	
% Macropores	21–53‡ (32±5)		21–36 (30±4)	
% Effective porosity			11–30 (19)	
SH			1.84–4.96 (2.57)	
σ	-6.08–7.83‡ (2.19±2.32)		1.17–6.98 (2.42±1.65)	
h_m (kPa)			5.07–81.7 (26.5)	
Denitrification rate ($\mu g\ N_2O$-N/kg soil/d)				-695.7–1590.5 (64.3)
DEA ($\mu g\ N_2O$-N/kg soil/d)				-977.6–944.4 (109.8)
NO_3^- (mg N/kg soil)				0–15.1 (3.02)
NH_4^+ (mg N/kg soil)				0.09–34.0 (5.43)

932
933 * Applies to all sampling sites used in mapping analysis
934 ** Applies to a set of 16 sampling points collected for an earlier study in 2005–2006. Due to flooding in 2007,
935 samples could not be collected in this portion of the site
936 ‖ Applies to the set of 18
937 ‡ Percent macropores for 2005-2007 samples were calculated using a regression-derived equation. Percent
938 macropores for 2009 were derived using variables derived from water retention curves.

Table 3. Final cluster center values and number of cases in each cluster using all nitrogen cycling data collected in August and September 2009. P-values for each variable are based on the ANOVA conducted to determine significant differences between the clusters.

ANOVA		Clusters				
p-value	Cluster ID	A	B	C	D	E
	# of cases	1	1	1	7	2
0.17	Denitrification rate (8/09)¶	-90.15	-47.79	5.44	25.94	98.03
0.001	Denitrification rate (9/09)¶	-695.7	-153.1	-6.87	57.59	319.23
<0.001	DEA (9/09)¶	-3.93	-977.7	774.6	49.93	-33.00
0.002	NO_3^- - 8/09ǂ	8,848	655	2,080	309	2,011
0.04	NO_3^- - 9/09ǂ	11,981	4,110	2,629	1,418	537
0.05	NO_3^- - DEA¶	15,103	-25	11,482	3,147	2,082
0.004	NH_4^+ - 8/09ǂ	1,799	15,610	916	1,561	14,863
0.001	NH_4^+ - 9/09ǂ	926	49,639	1,798	2,560	17,811
NS	NH_4^+ - DEA¶	2,650	12,964	915	2,106	15,965

¶ In μg N_2O-N kg $soil^{-1}$ d^{-1}; ǂ In μg N kg $soil^{-1}$

Table 4. Final cluster center values and number of cases in each cluster using intact core denitrification rates and select soil variables from intact cores collected in August and September 2009. P-values for each variable based on the ANOVA conducted to determine significant differences between the clusters are reported in the first column (NS=not significant, or p>0.2). Results of the cluster analysis (cluster center values, number of cases in each cluster) did not change when the analysis was re-run with only significant variables in the cluster analysis. Cluster center values of denitrification rates for both dates were regressed against cluster center values of each variable below; resulting R^2 and p values are reported in the last column (NO_3^- on both dates was pooled for the regression).

		Clusters					
ANOVA		A	B	C	D	R^2	p-value
p-value	# of cases	1	5	7	1		
<0.001	Denitrif rate (9/09)¶	-695.7	-38.59	70.19	469.1		
0.004	Denitrif rate (8/09)¶	-90.15	-16.40	31.87	171.1		
<0.001	σ	6.58	1.98	1.87	1.57	0.694§	0.05
0.15	% macropores	24	30	31	35	0.693§	0.05
NS	Elevation (m)	3.66	3.14	2.66	1.28	0.676§	0.06
0.02	NO_3^- - 9/09ǂ	11,981	4,114	626	-66	0.620	0.02
0.13	NO_3^- - 8/09ǂ	8,848	4,940	934	125		
0.07	h_m	52.62	12.27	26.69	30.51	0.593§	0.10
NS	MPS	0.08	0.09	0.05	0.03	0.582§	0.11
NS	% effective porosity	13	22	19	22	0.553	0.03
NS	% clay	6	5	15	5	0.533§	0.15
NS	σ_p	7.81	7.77	9.92	5.61	0.518§	0.16
0.05	SH_p	3.29	3.13	2.18	2.14	0.481§	0.06
NS	SH	5.41	5.59	4.61	4.52	0.365	0.11

¶ ln μg N_2O-N kg $soil^{-1}$ d^{-1}; ǂ ln μg N kg $soil^{-1}$; § Quadratic model

Table 5. Final cluster center values and number of cases in each cluster using potential denitrification rates and select soil variables from cores collected in September 2009. P-values for each variable based on the ANOVA conducted to determine significant differences between the clusters are reported in the first column (NS=not significant, or p>0.2). Results of the cluster analysis (cluster center values, number of cases in each cluster) did not change when the analysis was re-run with only significant variables in the cluster analysis. Cluster center values of denitrification rates for both dates were regressed against cluster center values of each variable below; resulting R^2 and p values are reported in the last column. Results of the cluster analysis (cluster center values, number of cases in each cluster) did not change when the analysis was re-run without these latter variables.

		Clusters					
ANOVA		A	B	C	D	R^2	p-value
p-value	# of cases	1	9	3	2		
<0.001	DEA¶	-977.6	17.29	279.8	774.57		
0.13	Elevation (m)	1.21	2.69	2.74	5.19	0.982§	0.13
NS	NO_3^- - DEA‡	-25	3,664	2,867	11,482	0.931§	NS
NS	SH_p	0.46	0.14	0.18	1.07	0.919§	NS
NS	% clay	10	12	14	2	0.886§	NS
NS	% macropores	31	30	32	29	0.871§	NS
NS	% effective porosity	23	19	21	14	0.836§	NS
NS	σ	1.43	2.92	1.52	2.56	0.742§	NS
NS	σ_p	8.72	9.73	9.11	5.32	0.636§	NS
NS	MPS	0.04	0.04	0.08	0.13	0.614	NS
NS	SH	4.66	5.10	4.46	4.97	0.227§	NS
NS	h_m	17.98	33.80	24.18	14.64	0.002	NS

¶ In μg N_2O-N kg $soil^{-1}$ d^{-1}; ǂ In μg N kg $soil^{-1}$; § Quadratic model

Figure 1

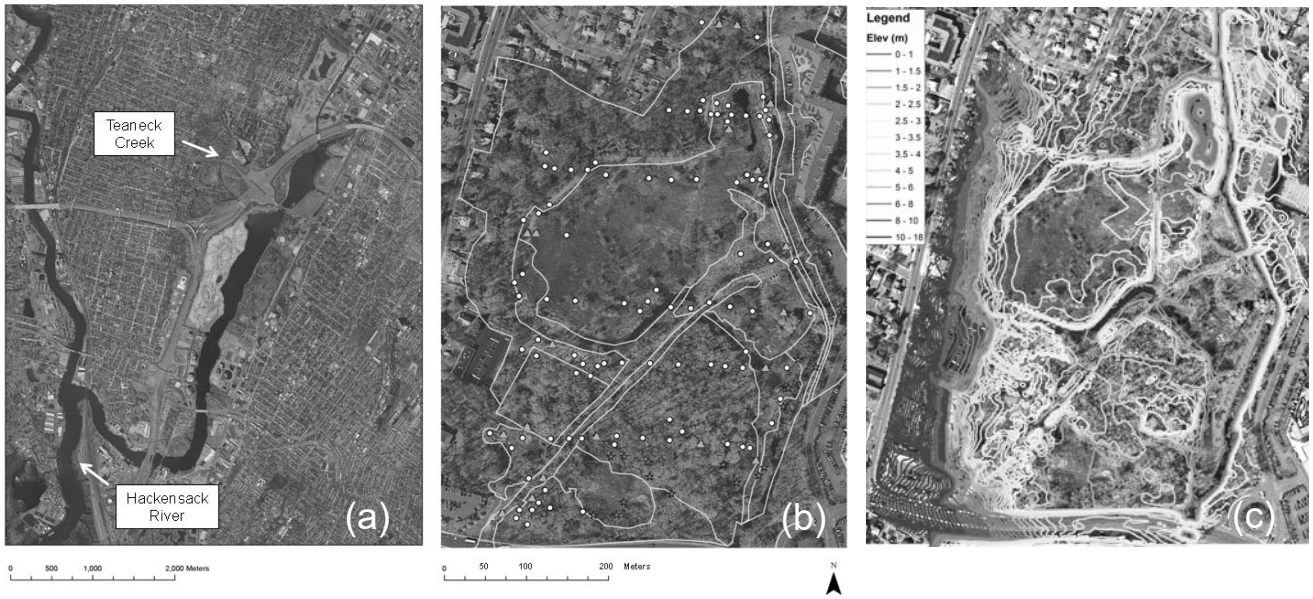

Figure 1. (a) The Hackensack River watershed and the Teaneck Creek Conservancy wetland site in 2007. **(b)** Data used to generate the denitrification hot spot map. Outlines in photo represent different land use areas digitized from a 1966 photograph (see supplemental material). White circles and blue triangles are sample locations collected in 2007 along transects. Blue triangles were also sampled for the denitrification and water retention study in 2009. Red stars are sample locations from sampling in 2005-06 that were used to augment the spatial datasets for organic matter and soil texture data. **(c)** Elevation map of the site.

Figures 2-5

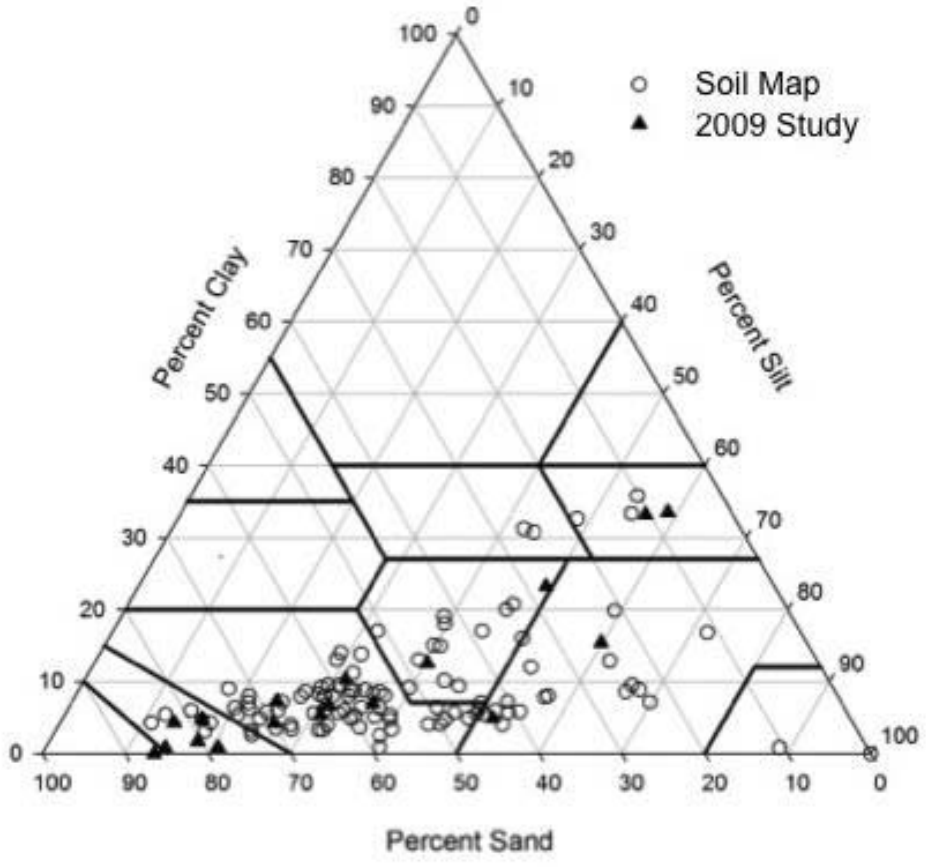

Fig. 2. Soil texture triangle of samples collected at the Teaneck site 2006–2007 (analyzed for texture and used to construct the soil map in Fig. 6). Eighteen samples (black triangles) were re-sampled in 2009 and used for measuring water retention curves, bulk density, denitrification rates, potential denitrification rates, and extractable inorganic nitrogen.

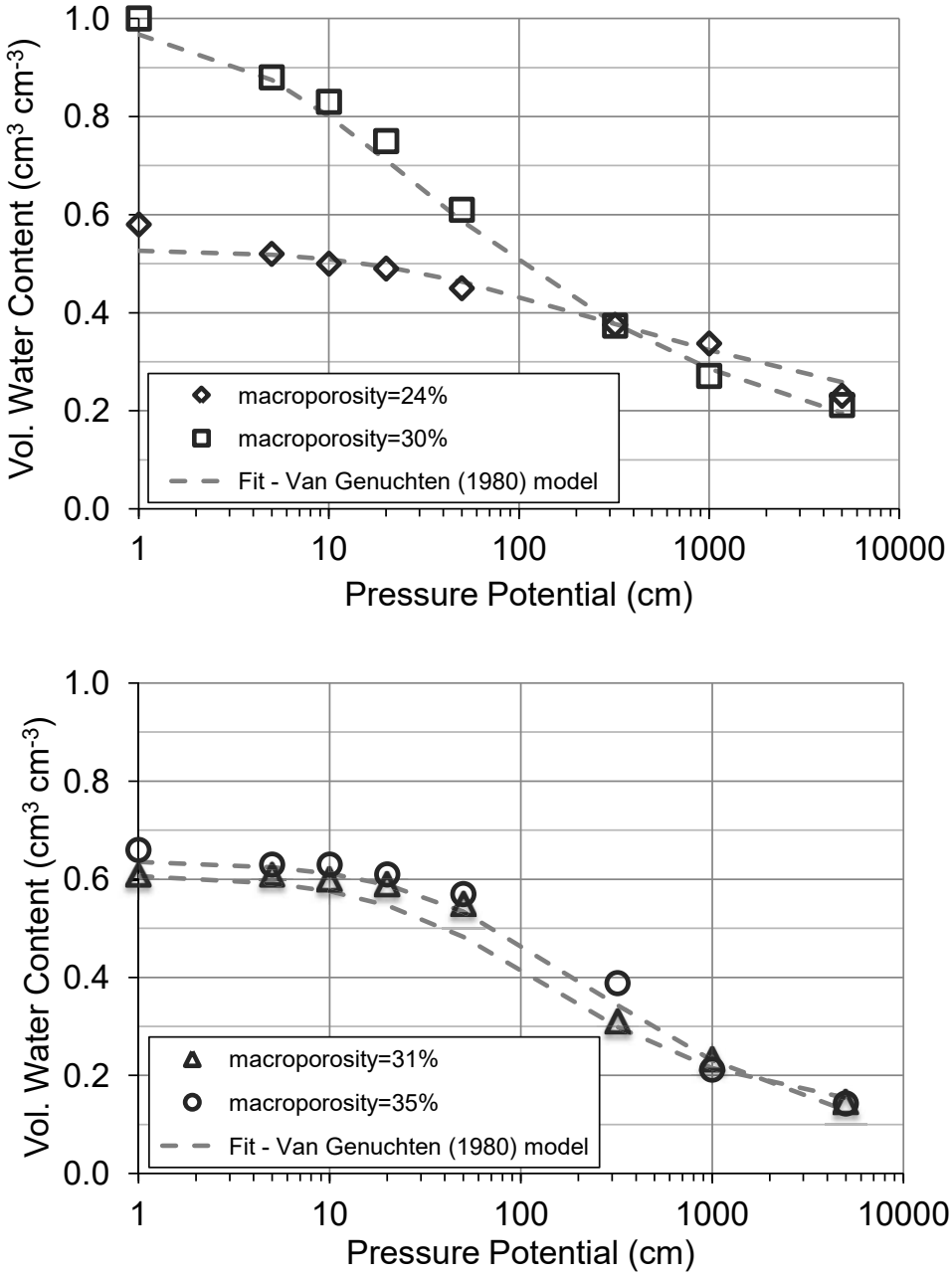

Fig. 3. Water retention curves generated for four samples representing collected from the Teaneck site and the van Genuchten model fit to each of these curves. The samples represent the four cluster center points of the intact core denitrification cluster analysis (shown in Table 4).

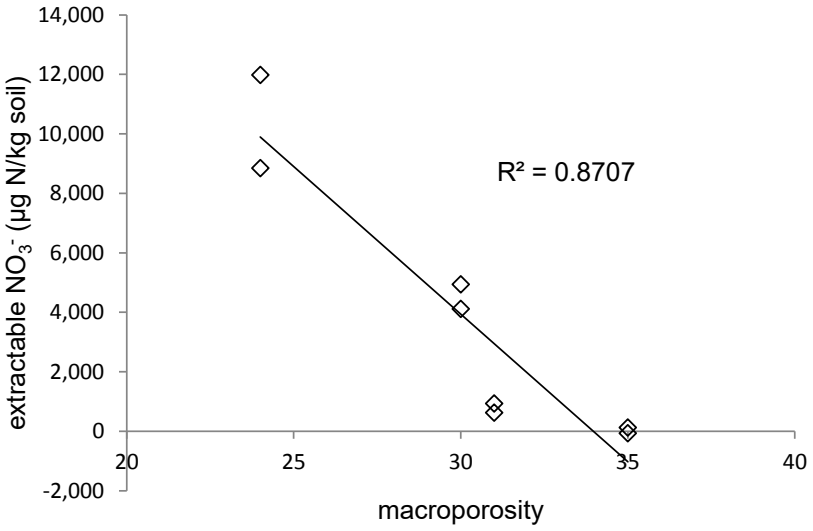

Fig. 4. Macroporosity as a predictor of extractable NO_3^- in intact core soil samples collected in August and September 2009. Values for each variable in the graph are cluster center values as determined by the cluster analysis shown in Table 3.

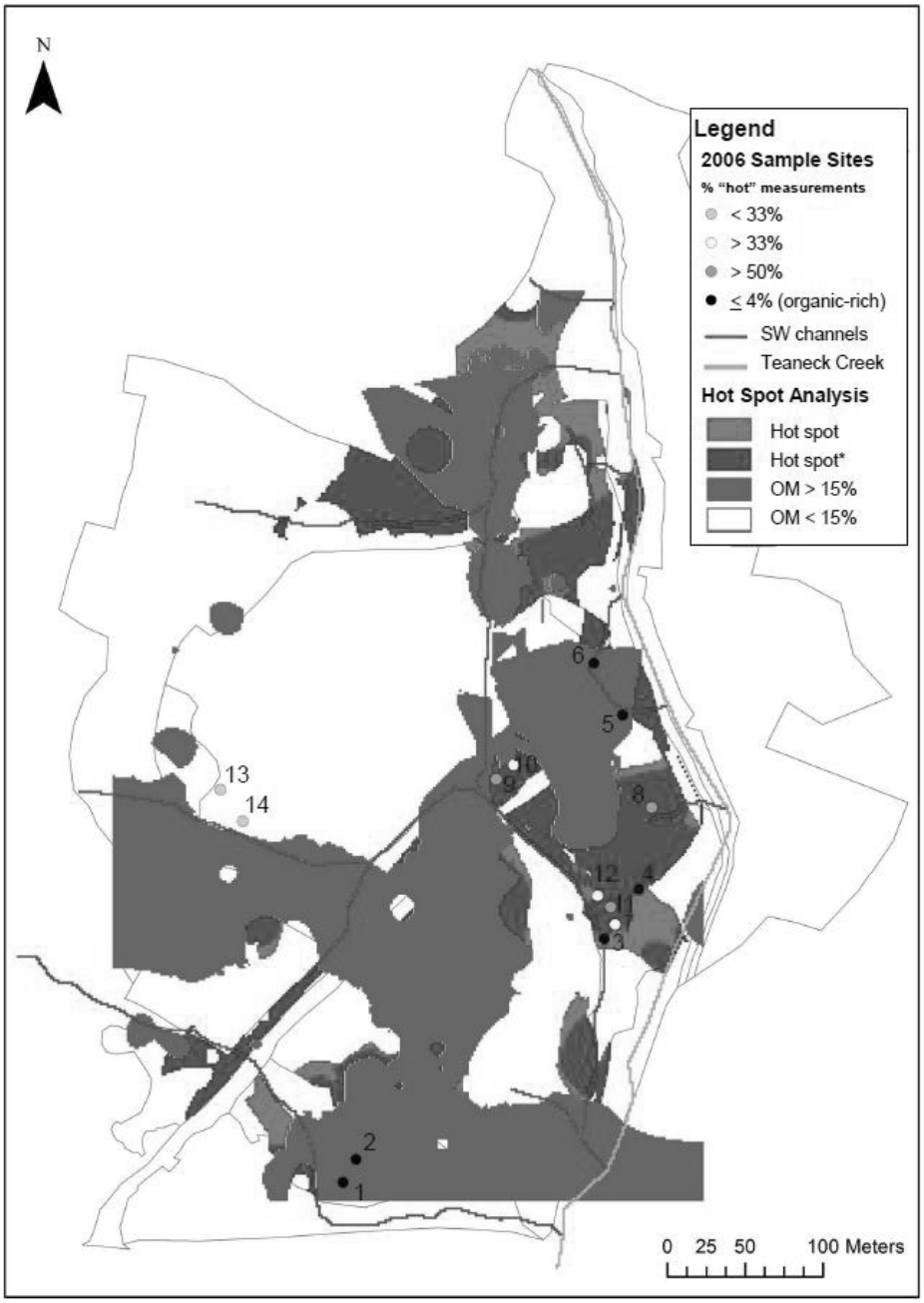

Fig. 5. Percent organic matter (OM), predicted hot spots of denitrification activity in soils, and stormwater (SW) channels at Teaneck Creek Conservancy. Hot spots (red) are areas with $\sigma<1.98$, macroporosity>0.30, organic matter<15%, and elevation<3.14 m. Hot spots* in dark red are areas meeting these criteria, but with σ values lower than 1.57 and macroporosities exceeding 0.35 (the minimum and maximum cluster center values for these variables, respectively – see Table 4). Points represent locations of intensive sampling for denitrification rate in 2006 (Palta et al., 2014). In Palta et al. (2014), a "hot" measurement was defined as denitrification rates exceeding the 75th percentile value of the data distribution.

Supplementary Material

Click here to download Supplementary Material for online publication only: SUPPLEMENTAL MATERIAL_22March2016.pdf